Supplementary Information for:

'The optimum fire window: applying the fire-productivity hypothesis to Jurassic climate states.'

Teuntje P. Hollaar*[1,2], Claire M. Belcher[1], Micha Ruhl[3], Jean-François Deconinck[4], Stephen P. Hesselbo[2,5]

[1]WildFIRE Lab, Global Systems Institute, University of Exeter, Exeter, EX4 4PS, UK
[2]Camborne School of Mines, Department of Earth and Environmental Sciences, University of Exeter, Penryn Campus, Penryn, TR10 9FE, UK
[3]Department of Geology, Trinity College Dublin, The University of Dublin, College Green, Dublin, Ireland
[4]Biogéosciences, UMR 6282 CNRS, Université de Bourgogne/Franche-Comté, 21000 Dijon, France
[5]Environment and Sustainability Institute, University of Exeter, Penryn Campus, Penryn, TR10 9FE, UK

*Corresponding author: t.p.hollaar@uu.nl

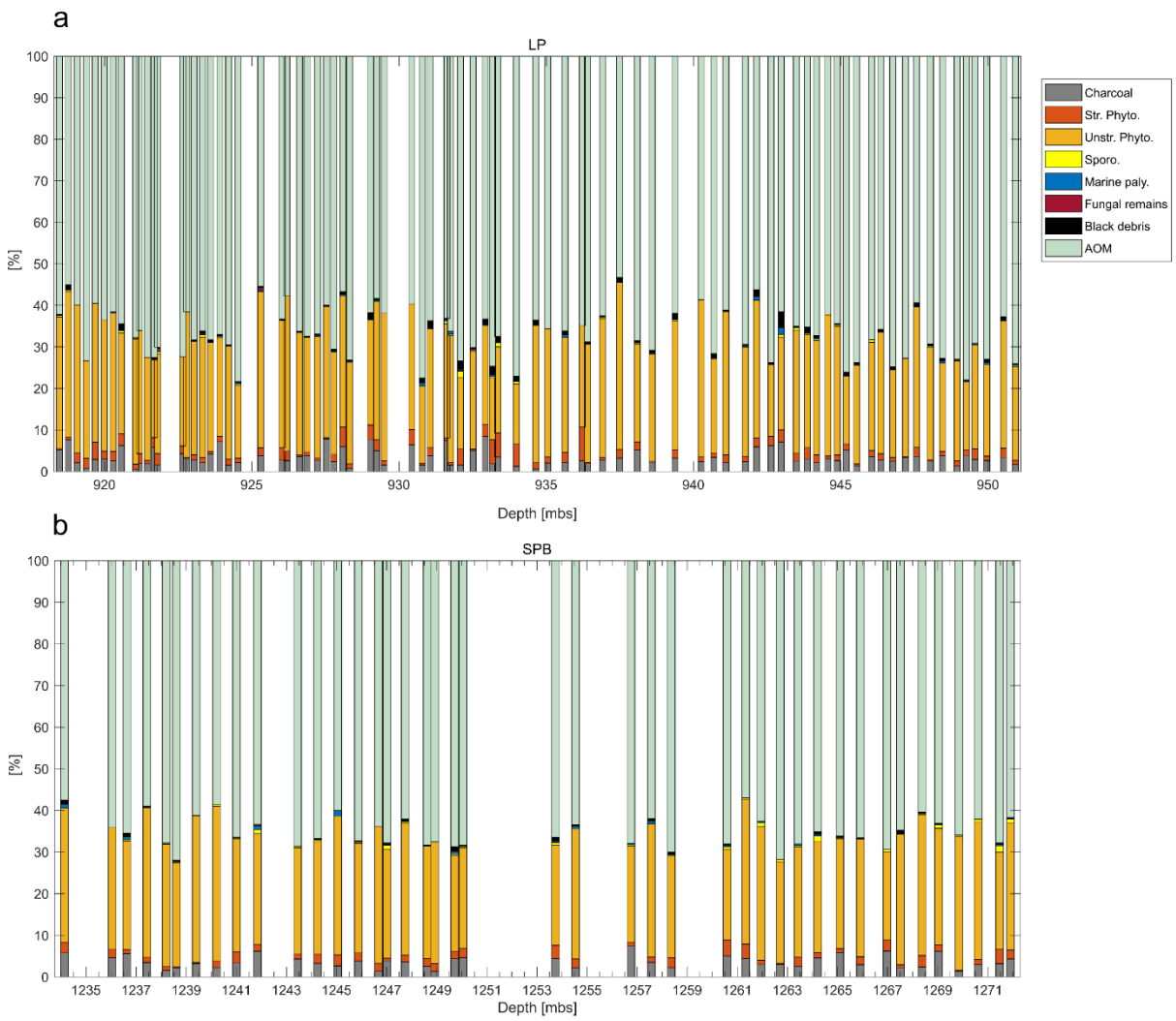

SI Fig. 1: Palynofacies of the (a) LP (published in Hollaar et al. (2021; 2023)) and (b) SPB studied intervals of the Mochras borehole. Relative abundance of the organic particle type identified under the reflective microscope. In each sample >300 organic particles were identified and grouped based on Oboh-Ikuenobe et al. (2005). Amorphous Organic Matter (AOM) is >50 % in all samples and constitutes the main bulk of the marine derived organic matter. This is followed by the group unstructured phytoclasts, which is of terrestrial origin. Only minor changes are observed in the relative abundance of terrestrial vs marine particulate organic matter and no abrupt or large shifts are observed.

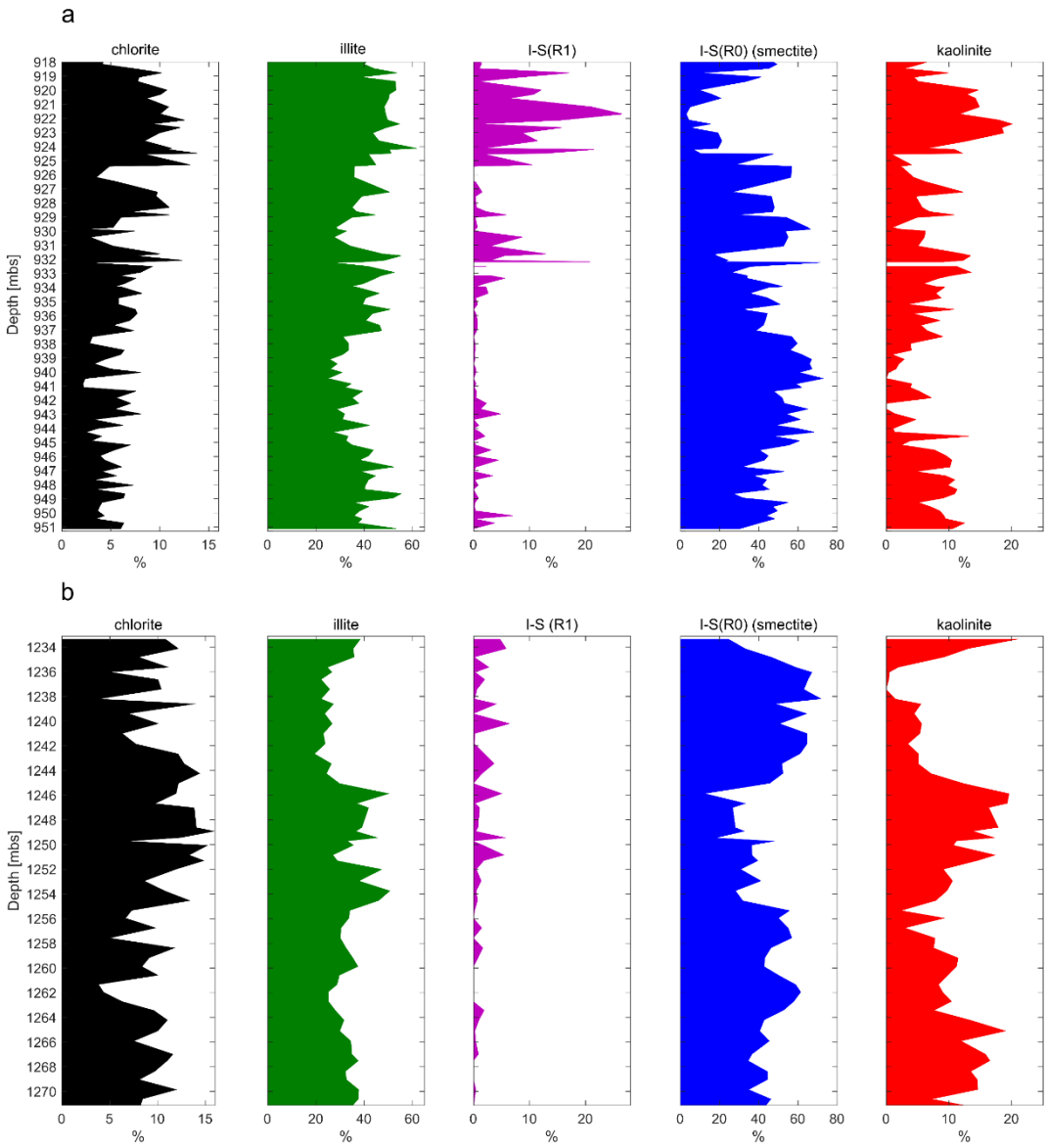

SI Fig. 2: Clay mineralogical abundance from the sediments of the LP and the SPB in the Mochras borehole. (a) The proportions of chlorite and illite-smectite mixed layers type R1 increase to the top of the record, coeval with illite and kaolinite. A long term opposite trend is observed in the abundance of smectite and kaolinite, in which kaolinite and illite co-vary (similar of the longer Pliensbachian clay mineralogy record of Mochras published in Deconinck et al. (2019). This indicates a climatic origin of the clay minerals (Deconinck et al., 2019) (results published in Hollaar et al. (2021; 2023)). (b) The clay mineralogical abundance record of the SPB studied interval. Chlorite is more abundant compared to the LP record. Smectite and kaolinite vary in parallel, however, the covariation of illite and kaolinite is less clear. I-S R1 type illite-smectite mixed layers are below the level of error detection (5 %) and are dismissed for interpretation in this record.

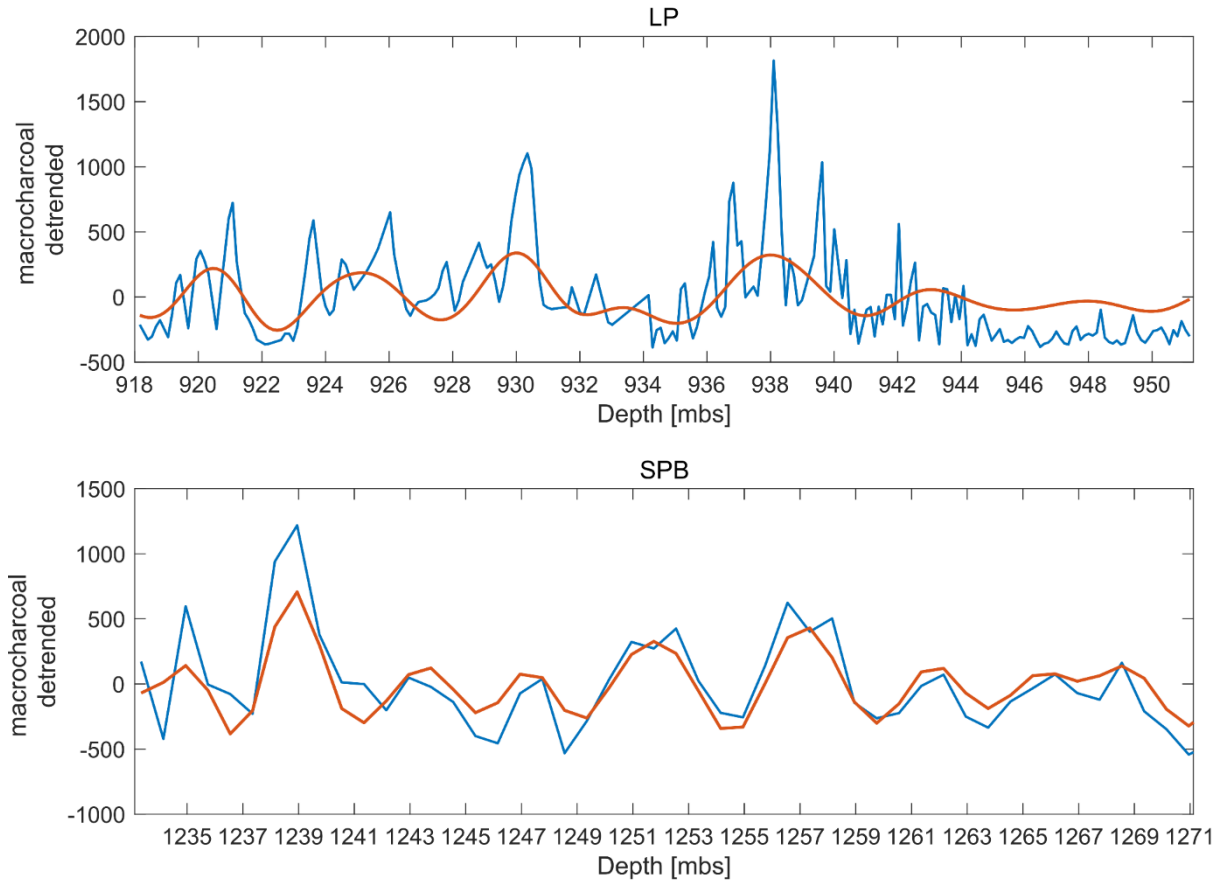

SI Fig. 3: Linear detrended macrocharcoal record and the 10.2 – 3.2 m filter. (a) The linear detrended macrocharcoal record of the LP interval in blue. The 10.2 – 3.2 m period is filtered out of the macrocharcoal record in Acycle. This broad filter resembles the 100 kyr periodicity in the depth domain (Ruhl et al., 2016). The number of peaks corresponds to the number of short eccentricity cycles in the studied interval found by Ruhl et al. (2016) and do capture the ~5 m bundles observed in the macrocharcoal record. (b) The linear detrended macrocharcoal record of the SPB studied interval in blue. The 10.2 – 3.2 m signal is filtered out of this charcoal record and plotted over the detrended charcoal record in orange. The individual peaks capture the ~5 m peaks in macrocharcoal observed in this record. Also, 9 peaks are observed, which is in agreement with Ruhl et al. (2016) who found 9 100 kyr eccentricity cycles for this interval.

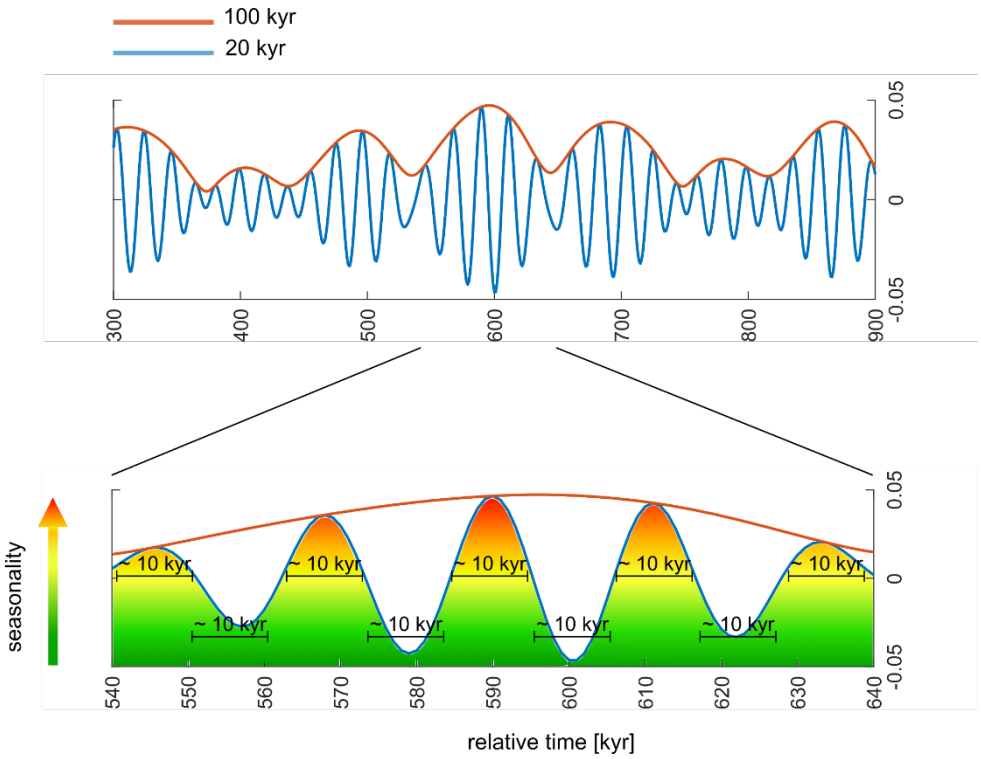

70

71

72 **SI Fig. 4:** Schematic image showing eccentricity modulation of the precession cycle, each precession
73 cycle contains ~ 10 kyr of minimum precessional forcing (equitable climate) and ~10 kyr of
74 maximum precessional forcing (extreme seasonal contrast). The ~20 kyr precession and ~100 kyr
75 eccentricity sine curves are derived from Laskar 2010d plotted in Acycle.

76

77